



## Crack initiation and fracture features of Fe–Co–B–Si–Nb bulk metallic glass during compression

S. Lesz, A. Januszka, S. Griner, R. Nowosielski

*Silesian University of Technology, Poland*

*sabina.lesz@polsl.pl, anna.januszka@polsl.pl, stefan.griner@polsl.pl, ryszard.nowosielski@polsl.pl*

**ABSTRACT.** The aim of the paper was investigation crack initiation and fracture features developed during compression of Fe-based bulk metallic glass (BMG). These Fe-based BMG has received great attention as a new class of structural material due to an excellent properties (e.g. high strength and high elasticity) and low costs. However, the poor ductility and brittle fracture exhibited in BMGs limit their structural application. At room temperature, BMGs fails catastrophically without appreciable plastic deformation under tension and only very limited plastic deformation is observed under compression or bending. Hence a well understanding of the crack initiation and fracture morphology of Fe-based BMGs after compression is of much importance for designing high performance BMGs.

The raw materials used in this experiment for the production of BMGs were pure Fe, Co, Nb metals and non-metallic elements: Si, B. The Fe–Co–B–Si–Nb alloy was cast as rods with three different diameters. The structure of the investigated BMGs rod is amorphous. The measurement of mechanical properties (Young modulus -  $E$ , compressive stress -  $\sigma_c$ , elastic strain -  $\varepsilon$ , unitary elastic strain energy -  $U_n$ ) were made in compression test. Compression test indicates the rods of Fe-based alloy to exhibit high mechanical strength. The development of crack initiation and fracture morphology after compression of Fe-based BMG were examined with scanning electron microscope (SEM). Fracture morphology of rods has been different on the cross section. Two characteristic features of the compressive fracture morphologies of BMGs were observed. One is the smooth region. Another typical feature of the compressive fracture morphology of BMGs is the vein pattern. The veins on the compressive fracture surface have an obvious direction as result of initial displace of sample along shear bands. This direction follows the direction of the displacement of a material. The formation of veins on the compressive fracture surface is closely related to the shear fracture mechanism. The results of these studies may improve the understanding on the fracture features and mechanisms of BMGs and may provide instructions on future design for ductile BMGs with high resistance for fracture.

**KEYWORDS.** Bulk metallic glasses; Compression test; Structure; Fracture morphology.



## INTRODUCTION

**M**etallic glasses (MGs) are poised to be mainstay materials for the 21<sup>st</sup> century due to the unique physical and chemical properties, which offers a great potential for application in industry, medicine, energy systems, microelectronics, aeronautics and many other fields. The first reported scientifically obtained metallic glass (MG) was the alloy Au<sub>75</sub>Si<sub>25</sub> produced at Caltech by Klement, Willens & Duwez in 1960, by extremely rapid cooling of the melted alloy [1]. In the 1960s, Chen and Turnbull developed amorphous alloys of Pd-Si-Ag, Pd-Si-Cu, and Pd-Si-Au [2]. Chen also fabricated an amorphous Pd-Cu-Si alloy with a diameter of up to 1 mm that could be considered to be a bulk metallic glass (BMG) [3]. A study of the mechanical properties of these novel materials was first reported in 1971 by Masumoto and Maddin [4]. In recent years a great expansion in the number of alloy compositions known to give bulk metallic glasses (BMGs) have occurred. The first Fe-based bulk metallic glasses (BMGs) were prepared in 1995 [5]. Since then, Fe-based bulk metallic glasses have been studied as a novel class of engineering materials, which have a good glass forming ability and soft magnetic properties [6,7]. For example, in 2004, Inoue et al. synthesized [(Fe<sub>x</sub>Co<sub>1-x</sub>)<sub>0.75</sub>B<sub>0.2</sub>Si<sub>0.05</sub>]<sub>96</sub>Nb<sub>4</sub> ( $x = 0.1$  and  $0.5$  at.%). BMGs exhibit good soft magnetic properties, as well as super-high fracture strength of 3000–4000MPa and ductile strain of 0.002 [6]. Bulk metallic glasses (BMGs) possess superior mechanical properties such as high strength and great elastic strain making them ideal candidates for structural applications. However, the poor ductility and brittle fracture exhibited in nearly all monolithic BMGs limit their structural application. Hence, a well understanding fracture morphology and mechanical properties is important for designing performance of BMGs.

The purpose of the paper was an investigation of the mechanical properties, structure and particularly fracture morphology of the Fe<sub>36</sub>Co<sub>36</sub>B<sub>19</sub>Si<sub>5</sub>Nb<sub>4</sub> bulk metallic glass (BMG) after compression.

## EXPERIMENTAL PROCEDURE

**T**he master alloy ingots with compositions of Fe<sub>36</sub>Co<sub>36</sub>B<sub>19</sub>Si<sub>5</sub>Nb<sub>4</sub> were prepared from the pure Fe, Co, Nb metals and non-metallic elements: Si, B, in an argon atmosphere. The alloy composition represents nominal atomic percentages. The investigated material was cast in form of rods with diameter of  $\phi=2, 3$  and  $4$  mm. According to Johnson, cooling rate achieved for an as-cast diameter  $R$  can be estimated as:  $T = 10/R^2$  (cm) [8]. Thus, the achieved cooling rate in the rod-shaped samples with  $\phi=2, 3$  and  $4$  mm in diameter could be estimated to be 1000, ~444 and 250 K/s. Obviously the smaller the as-cast diameter, the larger the cooling rate is achieved. The rods were prepared by the pressure die casting.

The following experimental techniques were used: X-ray diffraction (XRD) phase analysis method to test the structure, scanning electron microscopy (SEM) to investigate fracture morphologies obtained after decohesion process in compression test. The XRD method has been performed by the use of diffractometer XRD 7, Seifert-FPM, with filtered Co-K $\alpha$  radiation. The morphology of fracture surfaces after decohesion process in compression test was examined by means of the scanning electron microscope (SEM) SUPRA 25, ZEISS.

The measurement of mechanical properties, like: Young modulus -  $E$ , compressive stress -  $\sigma_c$ , elastic strain -  $\varepsilon$ , unitary elastic strain energy -  $U_u$ , were made in compression test. Compression tests for bulk metallic glasses were performed on ZWICK 100 testing machine at a strain rate of  $5 \times 10^{-4}$  s<sup>-1</sup>, at room temperature. For each group, five specimens were tested, and averaged data were used.

## RESULTS AND DISCUSSION

**I**t was found from the obtained results of structural studies performed by X-ray diffraction that diffraction pattern of surface rods with  $\phi=2, 3$  and  $4$  mm in diameter of Fe<sub>36</sub>Co<sub>36</sub>B<sub>19</sub>Si<sub>5</sub>Nb<sub>4</sub> alloy consists of a broad diffused halo typical for the amorphous phase (Fig. 1). The mechanical properties of samples, including Young's modulus -  $E$ , compressive stress -  $\sigma_c$  and elastic strain -  $\varepsilon$ , unitary elastic strain energy -  $U_u$ , are listed in Tab. 1 and Fig. 2.

As shown in the Fig. 2, the Fe<sub>36</sub>Co<sub>36</sub>B<sub>19</sub>Si<sub>5</sub>Nb<sub>4</sub> BMG exhibits elastic strain -  $\varepsilon$  of 0.75 to 0.94%. Young's modulus -  $E$  and compressive stress -  $\sigma_c$ , unitary elastic strain energy -  $U_u$  of the glassy alloy rods are in the range of 105-191 GPa, 790 - 1794 MPa, 17-25 kJ/m<sup>2</sup>, respectively. The values of unitary elastic strain energy -  $U_u$  decrease with the increasing diameter

of rods and are 25, 21 and 17 kJ/m<sup>2</sup> for the samples with diameters of  $\phi=2, 3$  and 4 mm, respectively. With the increase of rod's diameter the Young's modulus and stress decrease, suggesting a soft trend. These changes are probably connected with changes of structure relaxation. In sample in form of rod with 4 mm, where cooling rate of rods during casting is lower, the structure is more relaxed. This indicates that cooling rate plays a significant role in the plasticity of metallic glasses.

The compressive fracture surfaces are shown in Figs. 3-5. Fracture morphology of rods has been different on the cross section. Two characteristic features of the compressive fracture morphologies of metallic glasses (MGs) were observed.

Diameters of rod samples, $\phi$ [mm]	Young's modulus, $E$ [GPa]	Compressive stress, $\sigma_c$ [MPa]	Elastic strain, $\varepsilon$ [%]	Elastic strain energy, $U$ [kJ/m <sup>2</sup> ]
2	191	1794	0.94	25
3	135	1117	0.83	21
4	105	790	0.75	17

Table 1: Compressive mechanical properties of samples of the Fe<sub>36</sub>Co<sub>36</sub>B<sub>19</sub>Si<sub>5</sub>Nb<sub>4</sub> BMGs rods used in compression test at room temperature.

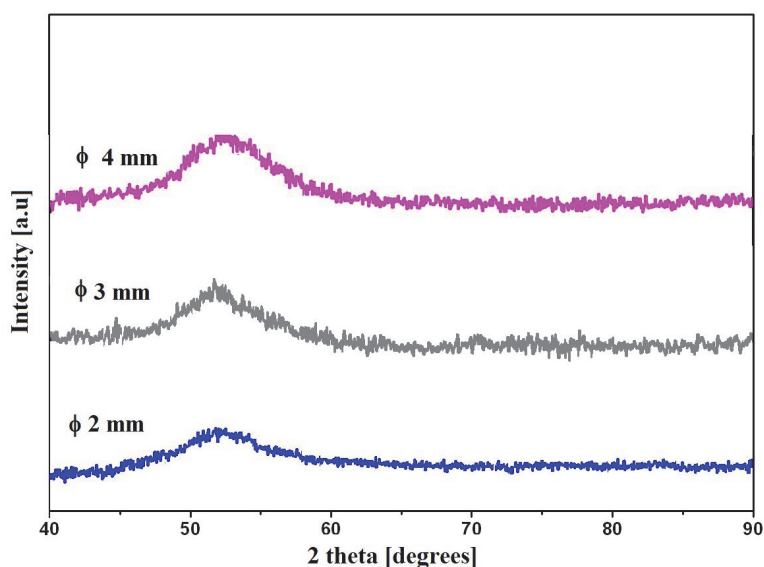


Figure 1: X-ray diffraction pattern of the Fe<sub>36</sub>Co<sub>36</sub>B<sub>19</sub>Si<sub>5</sub>Nb<sub>4</sub> BMGs rods with diameters of  $\phi=2, 3$  and 4 mm.

One is the smooth region, as shown in Figs. 3a,c,d, 4a,b,c,d,e, 5a,b. Another typical feature of the compressive fracture morphology of MGs is the vein pattern, as shown in Figs. 3a,b,c,d, 4a,c,d,e,f, 5c,d. The presence of these fracture morphologies indicates that the Fe-based BMG of this study classifies itself as a brittle amorphous material.

Figs. 3a-d show the SEM images of the fracture morphology of Fe<sub>36</sub>Co<sub>36</sub>B<sub>19</sub>Si<sub>5</sub>Nb<sub>4</sub> alloy rod with diameter of  $\phi=2$  mm after compressive fracture. Fig. 3a shows a main view of the 2 mm diameter BMG sample. The fracture surface of this sample consists of a smooth and vein pattern regions. Fig. 3b shows image of fracture outside surface, there are vein patterns and many cracks. The veins on the compressive fracture surface have an obvious direction probably compatible with direction of plastic strain. Fig. 3c shows an image of fracture of near the core of rod with smooth and vein pattern regions. Extensive cracks perpendicular to the fracture surface (in Fig. 3b) and rare small cracks within the veinlike pattern fracture (in Fig. 3c,d) can be observed. The well-developed fracture surface is observed for rods with a diameter of  $\phi=2$  mm. The fracture surface of rods with the diameter of  $\phi=3$  mm do not exhibit veinlike pattern in a region of rod core. The fracture surface is small-developed, nearly smooth. Only the edge of the rod the fine vein pattern morphology is observed. It is very interesting that angles between deep cracks formed and surface of the decohesion are from 68° to nearly 90° in relation to crack propagation direction.

Investigations of fractures of the  $\text{Fe}_{36}\text{Co}_{36}\text{B}_{19}\text{Si}_5\text{Nb}_4$  alloy rods with  $\phi=3.0$  mm in diameter showed similar morphology, as shown in Figs. 4a-f. Rare small cracks in the rods with  $\phi=3$  mm can be seen, like in the rods of  $\phi=2$ mm.

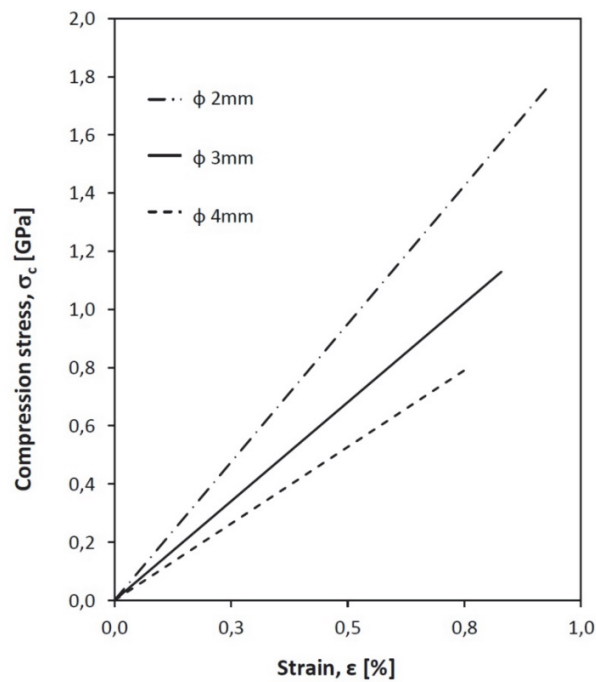


Figure 2: Compressive stress-strain curves of the  $\text{Fe}_{36}\text{Co}_{36}\text{B}_{19}\text{Si}_5\text{Nb}_4$  BMGs rods with diameters of  $\phi=2,3$  and 4 mm.

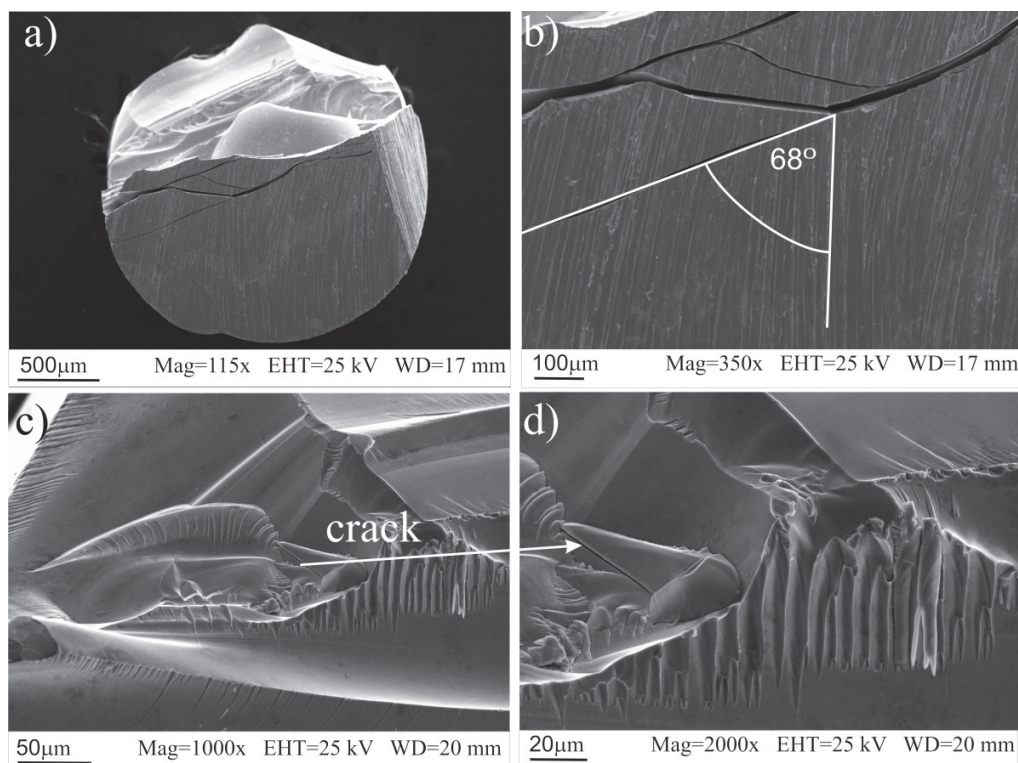


Figure 3: SEM images of the fracture morphology of  $\text{Fe}_{36}\text{Co}_{36}\text{B}_{19}\text{Si}_5\text{Nb}_4$  alloy rod with diameter of  $\phi=2$  mm after compressive fracture; a – main view: smooth and vein pattern regions, b – image of fracture outside surface, vein patterns, many cracks c – image of fracture of near the core of rod, smooth and vein pattern regions, clear crack, d – image of (c) at higher magnification. White arrow indicates the crack (c,d).

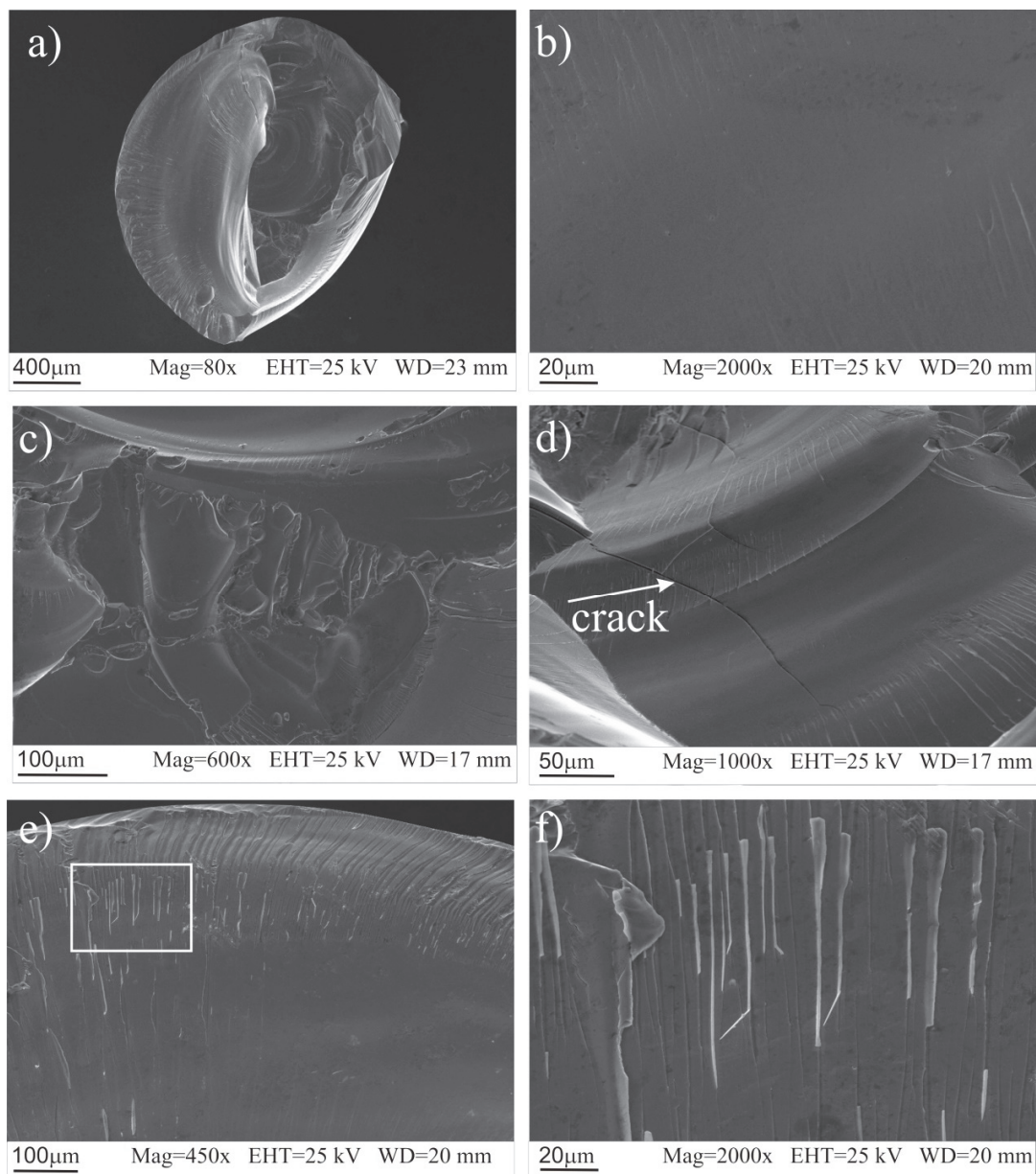


Figure 4: SEM images of the fracture morphology of Fe<sub>36</sub>Co<sub>36</sub>B<sub>19</sub>Si<sub>5</sub>Nb<sub>4</sub> alloy rod with diameter of  $\phi=3$  mm after compressive fracture; a – main view: smooth and vein pattern regions, b – image of fracture near the core of rod, smooth patterns, c, d – image of fracture near the core of rod, smooth and vein pattern regions, crack is indicated by arrow (d), e, f – image of fracture outside surface, vein and smooth patterns, f – image showing veins, as indicated by the rectangle in (e) at higher magnification.

The fracture surface of Fe<sub>36</sub>Co<sub>36</sub>B<sub>19</sub>Si<sub>5</sub>Nb<sub>4</sub> rod with diameter of  $\phi=4$  mm after compressive fracture consists of flat region with fine veins pass to the brittle crack region with extended surface, as shown in Fig. 5a. Fig. 5b shows the image of fracture near the core of rod. There are smooth and vein patterns. The fracture surface of rods with  $\phi=4$  mm does not exhibit another cracks extended to the material core besides the main fracture with the well-developed surface.

Fig. 5c shows the image of fracture outside surface with vein patterns regions. Magnified veins from the area as pointed in Fig. 5c was shown in Fig. 5d. The veins on the compressive fracture surface have an obvious direction as result of initial displace of sample along shear bands. This direction follows the direction of the displacement of a material.

As shown in Fig. 5d, the angles between the primary crack propagation direction and a region of secondary cracks is 60°. Presumably it is the effect of the change of the crack propagation direction. It influences the microstructure in areas showing the change of the direction of fine veins. The formation of veins on the compressive fracture surface is closely related to the shear fracture mechanism [9]. It seems that the fracture surface is independent on a strength level [10].

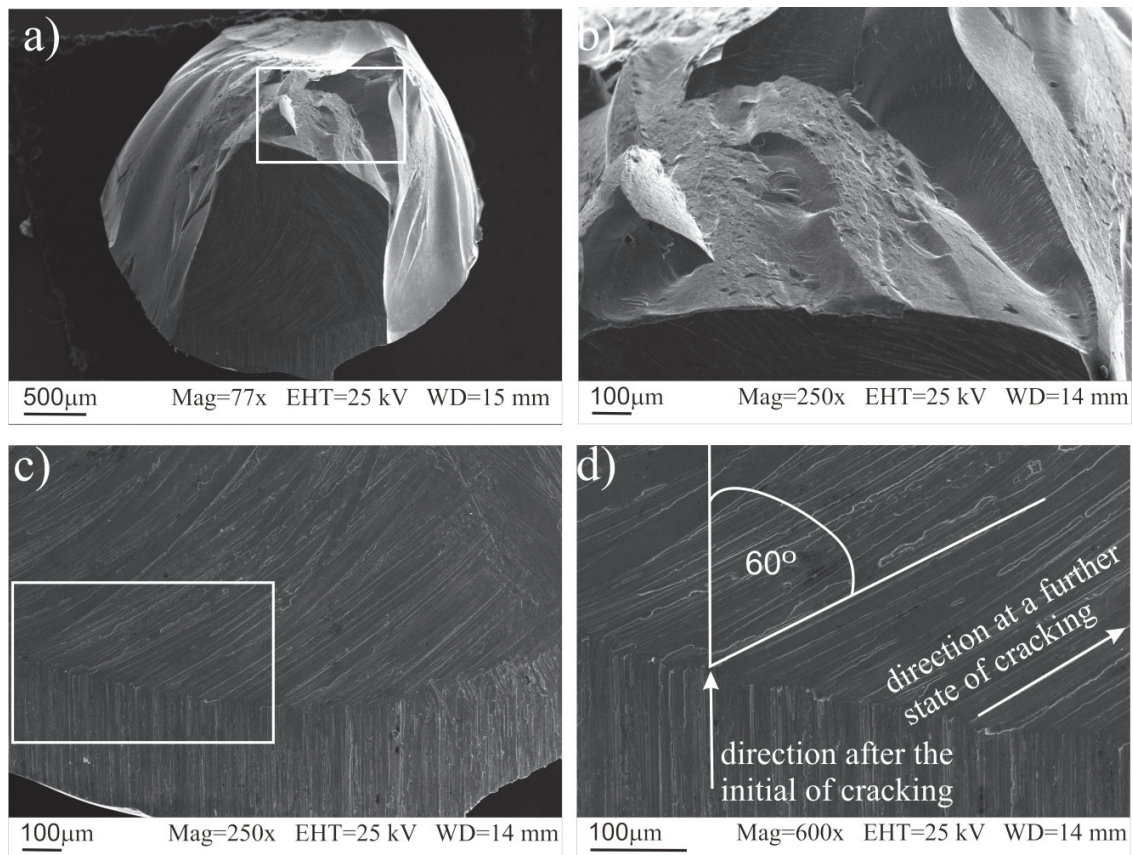


Figure 5: SEM images of the fracture morphology of Fe<sub>36</sub>Co<sub>36</sub>B<sub>19</sub>Si<sub>5</sub>Nb<sub>4</sub> alloy rod with diameter of  $\phi=4$  mm after compressive fracture; a – main view: vein and smooth pattern regions, b – image of fracture near the core of rod, smooth and vein patterns, c, d – image of fracture outside surface, vein patterns, d – magnified veins from the area as point in (c). White arrows indicate the direction after the initial of cracking and direction at a further state of cracking.

## CONCLUSIONS

The structure of surface rods with  $\phi=2, 3$  and 4 mm in diameter of Fe<sub>36</sub>Co<sub>36</sub>B<sub>19</sub>Si<sub>5</sub>Nb<sub>4</sub> alloy is amorphous. The Fe-based BMG rods exhibits elastic strain –  $\varepsilon$ , Young's modulus -  $E$ , compressive stress -  $\sigma_c$  and unitary elastic strain energy –  $U_b$ , of 0.75 to 0.94 %, 105 to 191 GPa, 790 to 1794 MPa and 17 to 25 kJ/m<sup>2</sup>, respectively.

Fracture morphology of rods after compressive fracture has been different on the cross section. Two characteristic features of the compressive fracture morphologies of metallic glasses (MGs) were observed in samples: smooth region and the vein pattern. The presence of these fracture morphologies indicate that the Fe-based BMG of this study classifies itself as a brittle amorphous material.

The results of these investigations suggest that the significant factor to control the structure, mechanical properties and fracture morphology of the Fe<sub>36</sub>Co<sub>36</sub>B<sub>19</sub>Si<sub>5</sub>Nb<sub>4</sub> BMG is cooling rate. Thus is factor has an instructional importance for the optimization of materials' performance.

## REFERENCES

- [1] Klement, W., R. H. Willens, Duwez, P., Non-crystalline structure in solidified gold–silicon alloys, *Nature*, 187 (1960) 869-870. DOI: 10.1038/187869b0.
- [2] Chen, H. S., Turnbull, D., Formation, stability and structure of palladium-silicon based alloy glasses, *Acta Metallurgica*, 17 (1969) 1021-1031. DOI: 10.1016/0001-6160(69)90048-0.



- [3] Chen, H. S., Thermodynamic considerations on the formation and stability of metallic glasses, *Acta Metallurgica*, 22 (1974) 1505-1511. DOI: 10.1016/0001-6160(74)90112-6.
- [4] Masumoto, T., Maddin, R., The mechanical properties of palladium 20 at/o silicon alloy quenched from the liquid state, *Acta Metallurgica*, 19 (1971) 725-741. DOI: 10.1016/0001-6160(71)90028-9.
- [5] Inoue, A., High strength bulk amorphous alloys with low critical cooling rates (overview), *Materials Transactions, JIM* 36(7) (1995) 866-875.
- [6] Shen, B., Inoue, A., Chang, C., Superhigh strength and good soft-magnetic properties of (Fe,Co)-B-Si-Nb bulk glassy alloys with high glass-forming ability, *Applied Physics Letters*, 85(21) (2004) 4911. DOI: 10.1063/1.1827349.
- [7] Lesz, S., Babilas, R., Nabialek, M., Szota, M., Dopisal, M., Nowosielski, R., The characterization of structure, thermal stability and magnetic properties of Fe-Co-B-Si-Nb bulk amorphous and nanocrystalline alloys, *Journal of Alloys and Compounds*, 509 (2011) 197-201. DOI: 10.1016/j.jallcom.2010.12.146.
- [8] Lin, X. H., Johnson, W. L., Formation of Ti-Zr-Cu-Ni bulk metallic glasses, *Journal of Applied Physics*, 78 (1995) 6514. DOI: 10.1063/1.360537.
- [9] Qu, R. T., Zhang, Z. F., Compressive fracture morphology and mechanism of metallic glass, *Journal of Applied Physics*, 114 (2013) 193504. DOI: 10.1063/1.4830029.
- [10] Inoue, A., Shen, B. L., Chang, C. T., Fe- and Co-based bulk glassy alloys with ultrahigh strength of over 4000 MPa, *Intermetallics*, 14 (2006) 936. DOI: 10.1016/j.intermet.2006.01.038.